Memory of Chirality in Flow Electrochemistry: Fast Optimisation with DoE and Online 2D-HPLC

Micol Santi, Jakob Seitz, Rossana Cicala, Tomas Hardwick, Nisar Ahmed and Thomas Wirth*[a]

Abstract: Amino acid derivatives undergo non-Kolbe electrolysis to afford enantiomerically enriched α-alkoxyamino derivatives through intermediate chiral carbenium ions. The products contain *N,O*-acetals which are important structural motifs found in bioactive natural products. The reaction is performed in a continuous flow electrochemical reactor coupled to a 2D-HPLC for immediate online analysis. This allowed a fast screening of temperature, electrode material, current, flow-rate and concentration in a DoE approach. The combination with online HPLC demonstrates that also stereoselective reactions can benefit from a hugely accelerated optimisation by combining flow electrochemistry with multidimensional analysis.

One of the key steps in research and development is process optimisation which focuses on maximising efficiency and productivity by minimising waste and costs. This is often time-consuming and does not always allow to comply with the twelve principles of green chemistry.[1] In the last decades, enabling technologies have offered a wide set of tools and time-saving devices such as continuous-flow systems[2] coupled with online analysis[3] and automated setups.[4]

Flow-microreactor technologies[5] allow a miniaturisation of reactions and an intensive high throughput screening in little time to then scale it back up once optimised for a pilot plant.[6]

Despite the many advantages, one of the main drawbacks of automated systems is the large amount of data that will be created in a short period of time. To overcome this issue, intelligent algorithms have been applied to self-optimising reactor systems[7] and modern statistical software for design of experiments (DoE) are now frequently used to perform such experiments.[8] Over the past 20 years DoE has found many applications in chemistry from reaction optimisation[9] to crystallisations,[10] and HPLC method development.[11]

The optimisation of enantioselective transformations can be challenging, especially as single-enantiomer drugs rather than racemates are important for drug validation.[12] Herein, we report an efficient way to quickly optimise asymmetric transformations *via* a DoE approach using a flow electrochemical microreactor coupled to an online multidimensional HPLC (Scheme 1).

Over the past decades, synthetic chemists have also renewed their interest in more "classic" areas of enabling technology such as electrochemistry as a more sustainable method to perform chemical transformations under mild reaction conditions.[13] Flow electrochemistry has recently also seen increased attention.[14]

We explore the enantioselective electrochemical reaction of *N*-arylcarbonylated amino acid derivatives to enantiomerically enriched alkoxylated amides. *N*-Acyl-*N,O*-acetals are important motifs present in natural products such as antiproliferative

pederin[15] and psymberin.[16] They are also interesting intermediates since they are stable but can be readily activated *in situ* for further chemical transformations.[17] Several methods have been reported towards *N,O*-acetals[18] including the oxidation of α-amino acids.[19]
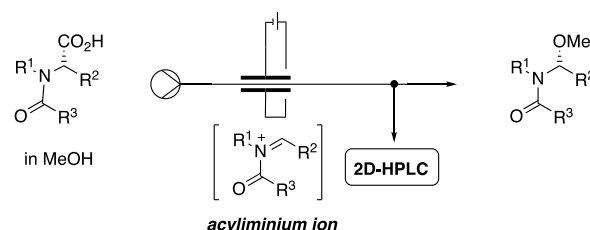
Scheme 1. Electrochemical oxidation of *N*-arylcarbonylated amino acid derivatives to chiral alkoxylated amides in a flow electro-microreactor.

The amino acid derivative shown in Scheme 1 undergoes a non-Kolbe electrolysis *via* memory of chirality through an acyliminium ion intermediate affording an enantiomerically enriched α-alkoxyamino compound. The first example of 'memory of chirality'[20] in acyliminium ion chemistry was reported in 2000 by Matsumura for the electrochemical oxidation of *N*-aryl serine derivatives **1** in methanol to afford optically active *N,O*-ketals **2**.[21] A change of the *N*-benzoyl group in **1a** to a bulkier 2-phenyl benzoyl protecting group (**1b**) using Pt as cathode and graphite as anode at –30 °C improved the enantioselectivity up to 80%. Very recently similar compounds have been employed in radical C – C -bond forming reactions where good enantioselectivities have been observed.[22]

1a, R = H
1b, R = Ph

2a, R = H, 69% yield, 39% *ee*
2b, R = Ph, 40% yield, 80% *ee*
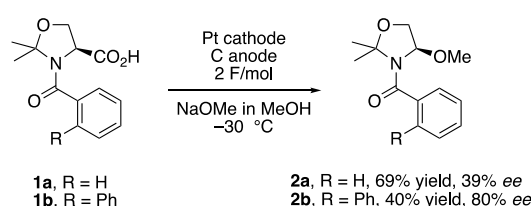
Scheme 2. First example of 'memory of chirality' on *N*-aryl serine derivatives **1** reported by Matsumura *et al.*[21]

The electrolysis of *N*-(2-phenyl)benzoyl proline derivative **3a** in a batch cell, however, afforded the methoxylated compound **4a** with poor yields and enantioselectivities (Table 1).

A large excess of base (10 equiv.) is needed to observe product **4a**, whereas without base the starting material **3a** was recovered completely (Table 1, entry 4). The stereoselectivity depends on the type of anode and on the temperature. In particular, a platinum anode is preferred over graphite especially when the reaction is performed at –30 °C affording **4a** in 40% *ee* (Table 1, entry 2).

We envisioned that the unstable acyliminium intermediate could be generated and used in a more controlled manner utilizing an electro-microreactor combined with online multidimensional

[a]   M. Santi, J. Seitz, R. Cicala, T. Hardwick, Dr. N. Ahmed, Prof. Dr. T. Wirth
School of Chemistry, Cardiff University
Main Building, Park Place, Cardiff, CF10 3AT (UK)
E-mail: wirth@cf.ac.uk

Supporting information for this article is given via a link at the end of the document.

analysis for faster optimisation. *S-trans* geometries for the acyliminium intermediate conformation have been suggested through substituent interactions[21b] and *s-cis* conformations have been calculated to be most stable in other cases,[21c] but on both occasions a shielding of the iminium moiety by the acyl substituent will cause the observed stereoselective reaction.

Initial screening of reaction parameters for the flow setup involved different electrode materials for the anodic oxidation (Pt, C, Pt on Nb, glassy C, C on PTFE, BDD) as well as various concentrations of **3a** and flow rates (see supporting information). Carbon-based anode materials showed better yields than platinum/platinum-coated or boron-doped diamond (BBD) except for the carbon-coated PTFE electrode. The glassy carbon electrode, despite the lower yield (37%), stands out for its impressive impact on the stereoselective nucleophilic attack leading to **4a** in 65% *ee*. Several materials were also screened for the cathode but lower or no conversions were observed, therefore the study was carried out using platinum as cathode material.

Table 1. Non-Kolbe electrolysis of **3a** to amide **4a** in an electrochemical batch cell (Volume: 5 mL).

Entry	Electrolyte (equiv.)	Anode	Temperature [°C]	Charge [F/mol]	Yield 4a [%]	ee 4a [%][a]
1	NaOMe (10)	Pt	25	2	47	30
2	NaOMe (10)	Pt	−30	2	15	40
3	NaOMe (10)	graphite	−30	2	1	18
4	none	Pt	−30	2	-[b]	-
5	NaOMe (10)	Pt	−30	4	dec.	-
6	NaOMe (10)	graphite	−30	4	dec.	-

[a] Determined by HPLC, OD-H column; [b] Only starting material was recovered, no current observed.

To identify the most significant parameters and two-factor interactions for this reaction a two-level fractional factorial design (FFD) 2^{5-1} was used with four numerical factors (concentration of starting material **3a**, flow-rate, charge and temperature), one categoric variable (type of anode) with yield and enantiomeric excess as responses.

Table 2. Levels (-1, 0, +1) of the five factors in the two-level fractional factorial design used by the factor generator E = A • B • C • D.

	Factor	Type	Unit	Level −1	Level 0	Level +1
A	concentration of **3a**	numeric	M	0.00625	0.00937	0.0125
B	anode material	categoric	-	graphite	-	glassy C
C	flow rate	numeric	mL/min	0.1	0.15	0.2
D	charge	numeric	F/mol	2	3	4
E	temperature	numeric	°C	−10	5	20

The 24 experiments were run in a random order within 24 h with 8 central points, 4 for each categorical level and through 2D-

HPLC online analysis both responses could be obtained within 15 minutes (see supporting information).

In theory, 2 F/mol of electricity should be sufficient for two consecutive single electron-transfer reactions. However, under these conditions the reaction did not go to completion (up to 76% HPLC yield, see Table S3 in the supporting information). When 4 F/mol of charge was used, the desired methoxylated amide **4a** was obtained in good (>80%) to quantitative yield with glassy carbon and graphite anodes. This is illustrated in the Pareto charts and 3D-surface plots shown in Figure 2.

The Pareto chart for the first response highlights the strong effects of charge (D) and anode material (B) on the yield (Figure 2a). The sharp slope on the 3D-surface plot for glassy carbon indicates the improvement on the yield when the number of electrons is increased from 2 to 4 F/mol (Figure 2c), which further improves passing from glassy carbon to graphite (see supporting information).
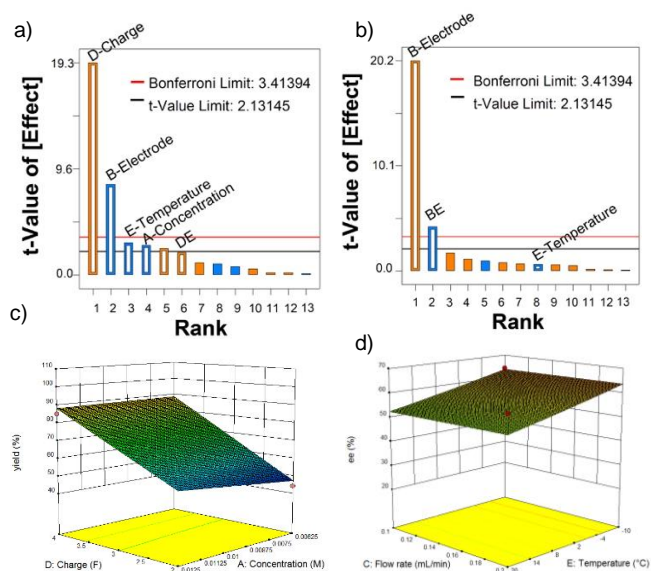

Figure 2. a) Pareto chart for the first response showing the effect of charge (D) and electrode type (B) on the yield of electrochemical oxidation of **3a** into **4a**; b) Pareto chart for the second response shows the effect of electrode type (B) and a moderate 2-factor interaction (BD) on the *ee*% of **4a**; c) 3D surface plot showing the yield for **4a** when glassy carbon is used at 20 °C and 0.2 mL/min; d) 3D surface plot showing the *ee*% for **4a** when glassy carbon is used with 4 F/mol on 0.0125 M solution of **3a**.

The cyclic voltammogram for **3a** (5 mM) in 0.1 M solution of *n*Bu₄NClO₄ in methanol is shown in Figure 3.
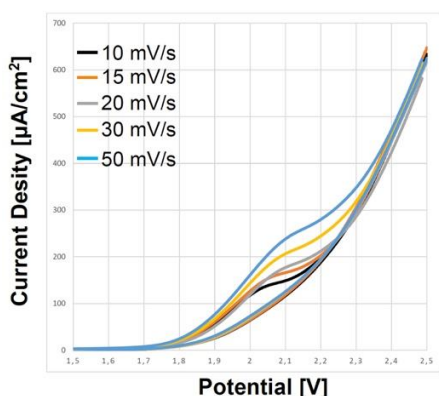
Figure 3. Cyclic voltammogram of substrate **3a** (5 mM) in 0.1 M *n*Bu₄NClO₄/ MeOH electrolyte (10 – 50 mV/s scan rate). Working electrode: glassy carbon electrode tip (3 mm diameter); Counter electrode: platinum wire; Reference electrode: Ag/AgCl in 3 M NaCl.

The oxidation peak of **3a** (+2.05 V vs Ag/AgCl) it is very close to the solvent oxidation peak.[23] This might indicate a competition between the two oxidations that could explain the excess of current needed.

Regarding the enantioselectivity, the most critical factor is the type of electrode used as anode (Figure 2b). In particular, when the reaction of **3a** was performed using glassy carbon at higher flow rate (0.2 mL/min), **4a** was afforded in moderate to good enantioselectivity (up to 70% *ee*, Figure 2d), whereas graphite showed only moderate selectivity (up to 31% *ee*). The unique ability of a carbon anode to promote the generation of carbenium ions in a Kolbe reaction is due to its paramagnetic centres which bind the initial radical and promote a second electron transfer.[24] Moreover, Matsumura *et al.* also observed an anode-dependent stereoselective non-Kolbe oxidation of L-threonine, suggesting an interaction between the carbenium ion and the anode surface.[21a]

Interestingly, the temperature (E) did not appear to be significant itself on the enantiomeric excess of this transformation, however, a moderate two-factor interaction between electrode and temperature (BE) was observed (Figure 2b).

Indeed, a different slope is observed for reactions performed at room temperature and at –10 °C using graphite and glassy carbon, respectively. This could be due to the non-linear behaviour of electrodes when other variables are changed. Graphite and glassy carbon behave differently at lower temperatures apparently influencing the stereocontrol of the nucleophilic attack. More experiments were performed to validate the observations and the best conditions were investigated with different anode materials as shown in Table 3.

Table 3. Further investigation and optimisation studies for the anodic oxidation of **3a** to amide **4a**.

Entry	Anode	Charge (F/mol)	T (°C)	4a [%][a]	4a ee [%][b]
1	glassy C	2	–10	60	70
2	glassy C	2	20	55	66
3	glassy C	4	20	77	60
4	glassy C	4	–10	81	66
5	Pt	4	20	4	49
6	Pt	4	–10	13	51
7	Pt on Nb	4	–10	14	48
8	Pt on Ti	4	–10	12	54
9	BDD	4	–10	54	60

[a] HPLC yield with *α,α,α*-trifluorotoluene as internal standard; [b] Determined by chiral HPLC.

When the reaction was performed at room temperature, product **4a** was obtained in similar yield and *ee* values than at a –10 °C, confirming the non-significance of the temperature itself (Table 3, entries 1 and 2).

However, when the charge was increased to 4 F/mol, despite the better yield of 71% a small loss in selectivity was detected (60% *ee*, entry 3). Both responses were maximised running the reaction at 0.2 mL/min, with 4 F/mol at –10 °C affording **4a** in 81% HPLC yield and 66% *ee* (entry 4). These optimised conditions were tested on Pt, Pt-coated and BDD anodes at both room temperature and –10 °C and similar *ee*-values were measured in all cases (see supporting information).

The distances of the electrodes were altered by using PTFE membranes with different thickness. A decrease of the thickness from 0.5 to 0.125 mm improved the yield (up to 86%) with only a small loss in stereoselectivity (see supporting information).

To better understand the effect involved into the stereoselective control, a full factorial model (FD) 2^3 was designed to study the electrolysis using glassy carbon as anode when only flow rate, charge and temperature were changed. A thin spacer (0.125 mm) was used to further reduce residence times and the voltage. In this full factorial design, a 3-factor interaction between charge, flow rate and temperature was observed for the enantioselectivity (see supporting information for all results). When the reaction was performed at 0.1 mL/min, the reaction was more difficult to control and to reproduce probably due to less efficient mixing. However, better enantioselectivities were obtained at higher flow rates, especially when the reactor was cooled to –5 °C suggesting a two-factor interaction between flow rate and temperature.

Once screening and optimisation steps were completed, the optimal conditions were used on a larger scale and the product collected over 1.5 h. The products **4b** – **4i** were isolated in moderate to good yields as shown in Figure 4.
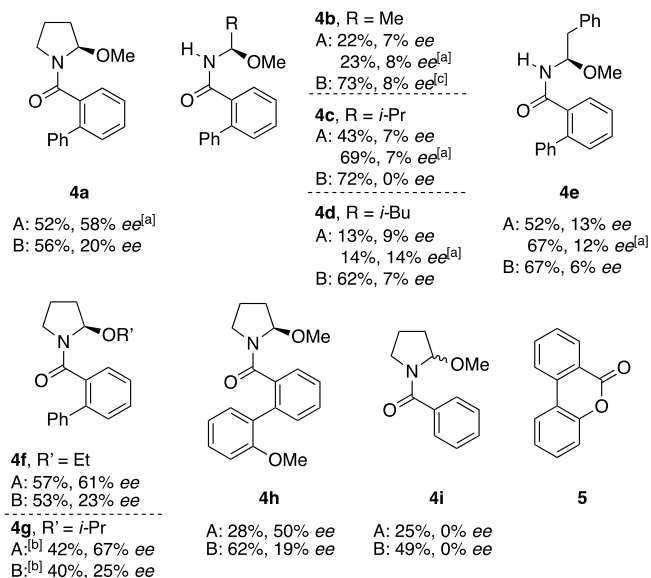
4a
A: 52%, 58% *ee*[a]
B: 56%, 20% *ee*

4b, R = Me
A: 22%, 7% *ee*
  23%, 8% *ee*[a]
B: 73%, 8% *ee*[c]

4c, R = *i*-Pr
A: 43%, 7% *ee*
  69%, 7% *ee*[a]
B: 72%, 0% *ee*

4d, R = *i*-Bu
A: 13%, 9% *ee*
  14%, 14% *ee*[a]
B: 62%, 7% *ee*

4e
A: 52%, 13% *ee*
  67%, 12% *ee*[a]
B: 67%, 6% *ee*

4f, R' = Et
A: 57%, 61% *ee*
B: 53%, 23% *ee*

4g, R' = *i*-Pr
A:[b] 42%, 67% *ee*
B:[b] 40%, 25% *ee*

4h
A: 28%, 50% *ee*
B: 62%, 19% *ee*

4i
A: 25%, 0% *ee*
B: 49%, 0% *ee*

5

Figure 4. Substrate scope for the electrochemical oxidation of *N*-protected amino-acids. The stereochemistry of **4a** was assigned according to literature.[25] The reaction were performed using a 0.013 M solution of **3a**. (A) Pt as the cathode and glassy carbon as anode at –10 °C or (B) graphite as anode at 20 ºC at 0.2 mL/min using 2 F/mol. [a] Reaction performed using a 0.05 M solution of starting material; [b] Reaction performed with 0.1 mL/min. [c] Product with (*S*)-stereochemistry obtained as major enantiomer.

A set of acyclic amino acid derivatives such as *N*-protected L-alanine, L-valine, L-leucine and L-phenylalanine were prepared and subjected to the electrochemical oxidation. Generally, graphite anodes afforded the desired products in better yields than glassy carbon, while glassy carbon provided higher enantioselectivities, as expected. We were delighted to observe the memory of chirality on not-constrained acyclic amino acids, albeit only moderate (up to 14% *ee*). When the oxidation was performed with glassy carbon anodes using L-alanine and L-leucine derivatives, the products **4b** and **4d** were isolated in low yields (22% and 13%, respectively) due to the formation of **5** as major side product (up to 30% yield). For L-valine and L-phenylalanine substrates, compound **5** was only detected in traces (< 9% yield) and the desired products **4c** and **4d** were isolated in 43% and 52% yield, respectively. The electrochemical cyclisation of 2-arylbenzoic acids to benzocoumarin derivatives of type **5** has recently been described.[26] A second recrystallisation was necessary to remove any traces of 2-arylbenzoic acid from **3b** and **3d**. The latter were then subjected to flow electrolysis (0.013 M) at 0.2 mL/min using glassy carbon as the anode. At room temperature products **4b** and **4d** were obtained in 80% and 62% yield with 10% and 7% *ee*, respectively.

For acyclic amino acids, the stereoselectivity increased with the steric demand of the side chain leading to **4b** – **e** in 7% – 13% *ee*. Interestingly, when the electrolysis on **3b** was performed with graphite as the anode, **4b** with (*S*)-absolute configuration was detected as the major isomer in 8% *ee*. Otherwise all products show (*R*)-configuration as previously established.[25] This observation strengthening the hypothesis that an interaction between the acyliminium ion and the electrode surface might be also involved in the memory of chirality. For a further scale-up

higher concentrated solutions (0.05 M) were used and it was possible to reproduce the same results without loss in reactivity or enantioselectivity.

When the electrolysis of **3a** was performed in ethanol or propan-2-ol instead of methanol, the desired products **4f** and **4g** were isolated in 57% and 42% yield with 61% and 67% *ee*, respectively. Finally, different protecting groups for amino acids were investigated. A more electron-rich biphenyl system as protecting group with a potential better stabilisation of the intermediate acyliminium ion did not lead to an improvement for the memory of chirality with **4h** isolated in 28% yield and 50% *ee.* Finally, to prove the importance of the biphenyl on the memory of chirality, a reaction was performed with benzoyl L-proline. As expected, **4i** was obtained as racemate irrespective of the type of anode used.

In summary, the enantioselective electrochemical oxidation of *N*-arylcarbonylated L-proline to enantiomerically enriched methoxylated amides was optimised using a DoE-approach in a flow electro-microreactor coupled to an online 2D-HPLC. The short reaction times combined with fast analysis time made a rapid screening of charge, electrodes, flow rate, concentrations, temperature and thickness of the PTFE membrane possible. We established an efficient method to intensively screen several parameters to quickly optimised asymmetric transformations and obtain high yields (up to 100%) and enantioselectivities (up to 70% *ee*) within a short period of time as well as reducing waste. Once optimised, the reaction was scaled-up and the products were isolated without loss in enantioselectivity. The optimal conditions were successfully tested on different alcohols and protecting groups. The methodology presented here might find useful application in the rapid optimisation of other stereoselective transformations.

Experimental Section

A solution of **3a** in methanol (0.05 M) was pumped through a Vapourtec Ion Electrochemical flow reactor (reactor volume = 0.6 mL, spacer 0.5 mm) at 0.2 mL/min using 2 F/mol (32 mA). An undivided cell arrangement was used with glassy carbon as anode and platinum as cathode (working surface area: A = 12 cm^2). The reactor was maintained constant at –10 °C. After reaching the steady state, the solution was collected for 90 min. The solvent was evaporated under *vacuum*, and the crude mixture was purified by flash column chromatography. The reaction stream was analysed online or offline using an Agilent 1290 Infinity 2D-LC. For the DoE Design Expert® 10 was used.

Acknowledgements

[1] P. T. Anastas, J. C. Warner, *Green chemistry: theory and practice*, Oxford University Press, Oxford, **1998**.

[2] a) M. B. Plutschack, B. Pieber, K. Gilmore, P. H. Seeberger, *Chem. Rev.* **2017**, *117*, 11796–11893; b) J. Britton, C. L. Raston, *Chem. Soc. Rev.* **2017**, *46*, 1250–1271.

[3] a) A. A. Folgueiras-Amador, K. Philipps, S. Guilbaud, J. Poelakker, T. Wirth, *Angew. Chem. Int. Ed.* **2017**, *56*, 15446–15450; b) N. Holmes, G. R. Akien, R.J. D. Savage, C. Stanetty, I. R. Baxendale, A. J. Blacker, B. A. Taylor, R. L. Woodward, R. E. Meadowse, R. A. Bourne, *React. Chem. Eng.* **2016**, *1*, 96–100; c) B. Ahmed-Omer, E. Sliwinski, J. P. Cerroti, S. V. Ley, *Org. Process Res. Dev.* **2016**, *20*, 1603–1614; d) S. T. R. Müller, A. Murat, D. Maillos, P. Lesimple, P. Hellier, T. Wirth, *Chem. Eur. J.* **2015**, *21*, 7016–7020.

[4] a) C. A. Shukla, A. A. Kulkarni, *Beilstein J. Org. Chem.* **2017**, *13*, 960–987; b) B. J. Reizman, K. F. Jensen, *Acc. Chem. Res.* **2016**, *49*, 1786–1796; c) V. Sans, L. Cronin, Chem. Soc. Rev. **2016**, *45*, 2032; d) D. E. Fitzpatrick, S. V. Ley, *React. Chem. Eng.* **2016**, *1*, 629–635.

[5] a) F. Fanelli, G. Parisi, L. Degennaro, R. Luisi, *Beilstein J. Org. Chem.* **2017**, *13*, 520–542; b) *Microreactors in Organic Chemistry and Catalysi*s, Ed. T. Wirth, Wiley, **2013**.

[6] S. T. R. Müller, A. Murat, P. Hellier, T. Wirth*, Org. Process Res. Dev.* **2016**, *20*, 495–502.

[7] a) V. Dragone, V. Sans, A. Henson, J. Granda, L. Cronin, *Nat. Commun.* **2017**, *8*, 15733; b) D. Cortés-Borda, K. V. Kutonova, C. Jamet, M. E. Trusova, F. Zammattio, C. Truchet, M. Rodriguez-Zubiri, F.-X. Felpin, *Org. Process Res. Dev.* **2016**, *20*, 1979–1987; c) V. Sans, L. Porwol, V. Dragone, L. Cronin, *Chem. Sci.*, **2015**, *6*, 1258–1264; d) M. Rasheed, T. Wirth, *Angew. Chem. Int. Ed.* **2011**, *50*, 357–358.

[8] a) V. Rosso, J. Albrecht, F. Roberts, J. M. Janey, *React. Chem. Eng.* **2019**, DOI: 10.1039/C9RE00079H; b) S. A. Weissman, N. G. Anderson, *Org. Process Res. Dev.* **2015**, *19*, 1605–1633.

[9] X. Tang, R. K. Allemann, T. Wirth, *Eur. J. Org. Chem.* **2017**, 414–418.

[10] H. Sato, S. Watanabe, D. Takeda, S. Yano, N. Doki, M. Yokota, K. Shimizu, *Org. Process Res. Dev.* **2015**, *19*, 1655–1661.

[11] J. Musters, L. van den Bos, E. Kellenbach, *Org. Process Res. Dev.* **2013**, *17*, 87–96.

[12] a) V. Farina, J. T. Reeves, C. H. Senanayake, J. J. Song, *Chem. Rev.* **2006**, *106*, 2734–2793; b) *Chirality* **1992**, *4*, 338–340.

[13] a) Q. Lin, L. Li, S. Luo, *Chem. Eur. J.* **2019**, *25*, 10033–10044; b) A. Wiebe, T. Gieshoff, S. Möhle, E. Rodrigo, M. Zirbes, S. R. Waldvogel, *Angew.*

Chem. Int. Ed., **2018**, *57*, 5594–5619; c) S. Möhle, M. Zirbes, E. Rodrigo, T. Gieshoff, A. Wiebe, S. R. Waldvogel, *Angew. Chem. Int. Ed.* **2018**, *57*, 6018–6041; d) M. Yan, Y. Kawamata, P. S. Baran *Chem. Rev.* **2017**, *117*, 13230.

[14] a) M. Elsherbini, T. Wirth, *Acc. Chem. Res.* **2019**, *in press*. DOI: 10.1021/acs.accounts.9b00497; b) A. A. Folgueiras-Amador, T. Wirth in *Flow Chemistry: Integrated Approaches for Practical Applications*, Eds: S. V. Luis, E. Garcia-Verdugo, RSC Publishing, **2019**, pp. 153–198; c) A. A. Folgueiras-Amador, T. Wirth, *Science of Synthesis, Flow Chemistry in Organic Synthesis*, **2018**, 147–189; d) K. Watts, A. Baker, T. Wirth, *J. Flow Chem.* **2014**, *4*, 2–11.

[15] T. Matsumoto, M. Yanagiya, S. Maeno, S. Yasuda, *Tetrahedron Lett.* **1968**, *9*, 6297–6300.

[16] N. Shangguan, S. Kiren, L. J. Williams, *Org. Lett.* **2007**, *9*, 1093–1096.

[17] a) H. Tohma, Y. Harayama, M. Hashizume, M. Iwata, Y. Kiyono, Y. Kita, *J. Am. Chem. Soc.* **2003**, *125*, 11235–11240; b) H. Tohma, Y. Harayama, M. Hashizume, M. Iwata, M. Egi, Y. Kita, *Angew. Chem. Int. Ed.* **2002**, *41*, 348–350; c) M. Sugiura, H. Hagio, R. Hirabayashi, S. Kobayashi, *J. Am. Chem. Soc.* **2001**, *123*, 12510–12517.

[18] a) M. Li, B. Luo, Q Liu, Y. Hu, A. Ganesan, P. Huang, S. Wen, *Org. Lett.* **2014**, *16*, 10–13; b) Y. Harayama, M. Yoshida, D. Kamimura, Y. Kita, *Chem. Commun.* **2005**, 1764–1766; c) G. Apitz, W. Steglich, *Tetrahedron Lett.* **1991**, *32*, 3163–3166.

[19] T. Iwasaki, H. Horikawa, K. Matsumoto, M. Miyoshi, *J. Org. Chem.* **1979**, *44*, 1552–1554.

[20] a) V. Alezra, T. Kawabata, *Synthesis* **2016**, *48*, 2997–3016; b) H. Zhao, D. C. Hsu, P. R. Carlier, Synthesis **2005**, 1–16; c) D. Seebach, D. Wasmuth, *Angew. Chem. Int. Ed.* **1981**, *20*, 971.

[21] a) Y. Matsumura, Y. Shirakawa, Y. Satoh, M. Umino, T. Tanaka, T. Maki, O. Onomura, *Org. Lett.* **2000**, *2*, 1689–1691; b) Y. Matsumura, T. Tanaka, G. N. Wanyoike, T. Maki, O. Onomura, *J. Electroanal. Chem.* **2001**, *507*, 71–74; c) Onomura, T. Maki, Y. Matsumura, *Org. Lett.* **2002**, *4*, 1875–1877.

[22] Y. Ozaki, T. Yamada, T. Mizuno, K. Osaka, M. Yamawaki, H. Maeda, T. Morita, Y. Yoshimi, *Tetrahedron* **2019**, *75*, 130493.

[23] T. Tajima, H. Kurihara, T. Fuchigami, *J. Am. Chem. Soc.* **2007**, *129*, 6680–6681.

[24] S. D. Ross, M. Finkelstein, *J. Org. Chem.* **1969**, *34*, 2923–2927.

[25] G. N. Wanyoike, Y. Matsumura, O. Onumura, *Heterocycles* **2009**, *79*, 339–345.

[26] L. Li, Q. Yang, Z. Jia, S. Luo, *Synthesis* **2018**, *50*, 2924–2929.

COMMUNICATION

Asymmetric transformations are quickly optimised using a DoE-approach with an electrochemical flow reactor attached to a 2D-HPLC. Cyclic and acyclic *N,O*-acetals were obtained from moderate to good yields and enantioselectivities. The highly reactive acyliminium ion serves as a chiral intermediate leading to the desired product with 'memorised' chirality (up to 70% *ee*) in a short reaction time.

chiral acyliminium intermediate
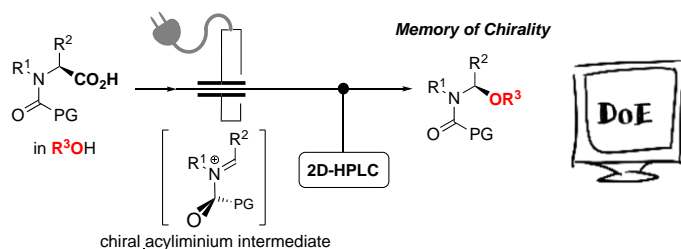
Micol Santi, Jakob Seitz, Rossana Cicala, Tomas Hardwick, Nisar Ahmed, Thomas Wirth*

Page No. – Page No.

Memory of Chirality in Flow Electrochemistry: Fast Optimisation with DoE and Online 2D-HPLC